Development and experimental evaluation of an automatic marker registration system for tracking of augmented reality

YAN Wei-da[1], YANG Shou-feng[1], ISHII Hirotake[1], SHIMODA Hiroshi[1] and IZUMI Masanori[2]

1. Graduate School of Energy Science, Kyoto University, Kyoto 606-8501, Japan
(yanweida@ei.energy.kyoto-u.ac.jp, yousyuhou@yahoo.co.jp, hirotake@energy.kyoto-u.ac.jp, shimoda@energy.kyoto-u.ac.jp)
2. FUGEN Decommissioning Engineering Center, Japan Atomic Energy Agency, Tsuruga 914-8510, Japan
(izumi.masanori@jaea.go.jp)

Abstract: In order to apply augmented reality in plant maintenance activities it is necessary to use real-time high accuracy tracking technology. One of the most efficient tracking methods is using paper-based markers and computing the relative position and orientation between a vision sensor (camera) and the markers through image processing and geometry calculations. In this method, the 3D-position of each marker is needed before tracking, but it is inefficient to measure all the markers manually. In this study, an automatic marker registration system was developed so as to measure the 3D-position of each marker automatically. The system is composed of a camera, a laser rangefinder and a motion base, which is used to control the pose of the laser rangefinder. A computer, connected to them, is used for controlling the system and for data transport. The results of the experimental evaluations show that the measurement takes about 21 seconds per marker and that the Root Mean Square Error (RMSE) of the position measurements is 3.5 mm. The feasibility evaluation of the system was conducted in Fugen nuclear plant. The results show that the system can largely reduce the preparatory workload of an AR application in a Nuclear Power Plant (NPP).

Keywords: Augmented Reality; Marker-based Tracking; Circular Marker; Automatic Registration; 3D-Position

1 Introduction

Augmented Reality (AR) expands the surrounding real world of the users by superimposing computer-generated information on the users' view [1, 2]. It represents information more intuitively than with legacy interfaces, such as paper-based instruction documents. AR is broadly used in many fields, such as medical, manufacturing, entertainment, etc. The car-manufacturer BMW uses AR as part of its car maintenance system [3], where an element needing repair is displayed in the worker's view. AR has successfully been used as an aid system for maintenance of control boxes [4]; where the operation information displayed in the HMD helped reducing human error and raising efficiency. As yet another example, Davison has used this technology to add imaginary furniture into a kitchen [5].

It is expected to apply AR to support NPPs maintenance activities so as to minimize human error and improve efficiency and safety. For practical applications of AR, a tracking method that measures the position and orientation of users in real time is indispensable. There are many tracking technologies that support AR, such as Global Positioning System (GPS), magnetic sensors, ultrasonic sensors and inertial sensors. But GPS is useful only outdoors, magnetic sensors and ultrasonic sensors are easily disrupted by metal instruments, and errors of inertial sensors increase over time [2]. Therefore, the only method suitable for a NPP's environment is a paper-based marker one. Square markers have been widely used for paper-based tracking, but only in short distance tracking [6-8]. In this study, since workers of a NPP are expected to move throughout capacious spaces, circular markers, which can be used in long distance tracking, were applied [9].

For tracking in capacious spaces, like those of NPPs, a great number of markers are necessary and the 3D-position of each marker must be measured before using the marker based method. Given that manual measurement is inefficient and highly subject to human error, in this study, an automatic marker

Received date :January 28，2010
(Revised date: February 19, 2010)

registration system was developed. This system can measure the 3D-position of a marker automatically and quickly, making it convenient and more accurate (minimizing human error). The system's performance evaluation of measurement accuracy and stability was conducted in a laboratory, whereas the feasibility evaluation was analyzed in a NPP.

2 A tracking method using paper-based markers and a camera

A circular marker was designed as shown in Fig.1. Each marker consists of one black outer circle with a thickness of 30% of the marker's radius, one white center circle with a radius equivalent to the 30% of the marker's radius and one middle circle between them, which consists of 10 black or white fans that represent an ID.

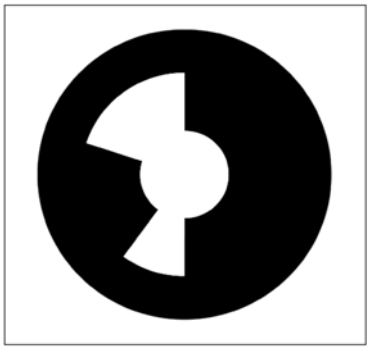

Fig.1 Circular marker.

The following steps describe the use of markers for tracking:

1) Users paste the markers around the environment and capture their images using a camera.
2) The ID and position of each marker on the images is recognized through image processing.
3) The relative position and orientation between the camera (users) and the markers is calculated using the PnP (Perspective N-Point Problem) method [10]. For this method, the 3D-position of each marker is necessary.

3 Development of the system

For practical applications in a NPP, an ideal system should be able to:

1) Measure the marker's 3D-positions as quickly as possible
2) Have enough accuracy and stability so as to apply AR in field work
3) Allow workers to master the operation of the system as soon as possible
4) Work with low-price hardware
5) Be set up even in narrow spaces
6) Work in an environment with obstacles

In the following paragraphs of this chapter, the components of the system and the realization algorithms of the system's functions will be described.

3.1 The system's profile

As shown in Fig.2, the system is composed of a camera, which has an interior motion base, a laser rangefinder, a motion base fixed under the laser rangefinder and a PC connected to them. The camera and the motion base are both fixed onto a tripod. The directions of the camera and the laser rangefinder are controlled from the PC through motion base controllers. Table 1 displays the capability of the hardware.

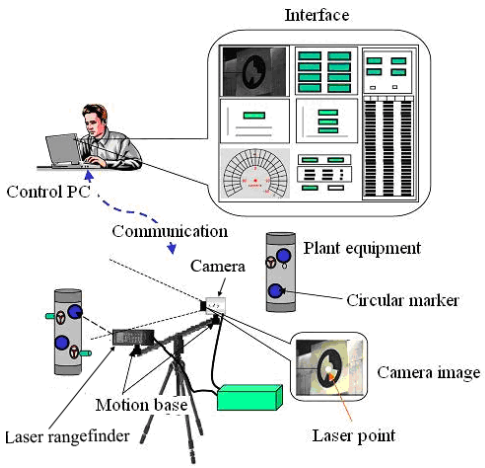

Fig. 2 Components of the system.

The system works as following:

1) The users select the world coordinate system (right hand system) and locate the fiducial markers (where marker No.1 is at origin, No.2 is at +X axis, and No.3 is at plane XOY).
2) The system is set up at a place where it can capture the images of all markers.
3) The system measures the 3D-position of each marker automatically.
4) The results are saved into a file, to be used later in the AR application.

The above's step 3) is automatically executed in the

Table 1 The system's hardware

Video camera	Type	Sony EVI-D30
	Video signal	NTSC
	Focus	5.4mm～64.8mm
	Horizontal angle of view	48.8°～4.3°
	Pan/Tilt	Horizontal ±100° Vertical±25°
	Control terminal	RS-232C
	Weight	1.2kg
Laser rangefinder	Type	Leica Geosystems DISTO Pro 4a
	Range	0.3m～40m
	Accuracy	Typical: ±1.5mm Max: ±2mm
	Φ Laser dot (at distance)	6/30/60mm (10/50/100m)
	Control Terminal	RS-232C
	Weight	0.44kg
Motion base	Type	Directed Perception PTU-D46-70
	Position resolution	0.012857°
	Max speed	60°/s
	Pan/Tilt	Horizontal ±159° Vertical -31°~+48°
	Control terminal	RS-232C
	Weight	1.5kg
PC	Type	ASUS M5N
	CPU	Pentium M 1.4GHz
	Memory	DDR333 768MB
	OS	Microsoft Windows XP Home Edition
	Weight	1.55kg

following way:

3-1) The camera rotates and captures images of its surrounding environment (controlled from the PC through motion base controllers) and, once the markers are recognized, the markers' positions are estimated.

3-2) The system changes the direction and zoom of the camera to enlarge a recognized marker's image at the center of the screen

3-3) Using the estimated result obtained in 3-1), the system points the laser rangefinder to the marker. Here the estimated results include large errors.

3-4) The two images captured, before and after the laser shooting, are compared in order to find the laser's dot.

3-5) The laser rangefinder shoots at the marker's center. Then, the relative 3D-position between the laser rangefinder and the marker is measured.

3-6) The information of the 3D-position is converted into the world coordinate system.

3-7) Repeat from 3-2) to 3-6) to measure next recognized marker.

Given that all the above steps, 3-1) to 3-7), are automatically controlled by a PC, the whole process is much more efficient and significantly less subject to human error than with a manual measurement. Additionally, if the fiducial markers in the world system are not removed, the system can be set up at any place where it can capture them. So, even in the event that some markers were not successfully measured, they can be measured again by changing the position of the system. (In this case, the 3 fiducial markers, No.1 to No.3, will have to be measured again.)

3.2 Markers' automatic measurement algorithm

3.2.1 Definition of coordinate systems

Different coordinate systems are defined as shown in Fig. 3. In this study, translation and rotation from system 1 to system 2 are represented as $\boldsymbol{T}_{12}$ and $\boldsymbol{R}_{12}$, respectively.

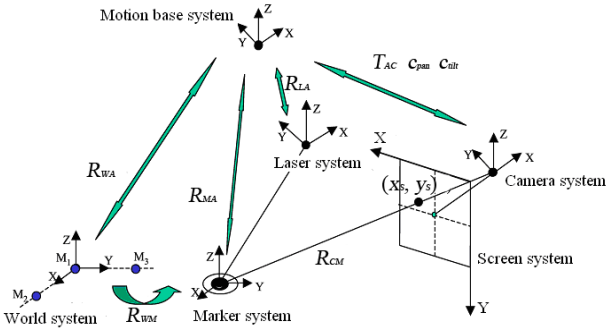

Fig. 3 Coordinate systems.

1) World system *W*. It is defined by 3 fiducial markers. (No.1, 2 and 3) The center of marker No.1 is the origin O, the direction from the center of No.1 to No.2 is the +X direction. The plane composed by the centers of the 3 fiducial markers is the XOY plane.

2) Motion base system *A*. For the motion base fixed under the laser rangefinder, the intersection of its pan and tilt axes is the origin, the up direction and front direction of its initial position is +Z and –X, respectively.

3) Laser system *L*. The projection of the origin of *A* on the rotation plane of the laser rangefinder is the origin. The directions of the axes are the same as in *A*.
4) Screen system *S*. In the image plane, the up-left corner is the origin, the right direction is +X and the down direction is +Y.
5) Motion base system *B*. For the camera's interior motion base, the intersection of its pan and tilt axes is the origin, the up direction and front direction of its initial position are +Z and –X, respectively.
6) Camera system *C*. The focal point of the camera is the origin, the direction from the center of the image plane to the origin is +X, the direction parallel to the X axis of *S* is +Y.
7) Marker system *M*. The marker's center is the origin. The border of two fans, which represent the first bit and the last bit of a marker's ID, respectively, is the X axis. The normal to the marker's plane is the Z axis.

In this study, the origins of *B* and *C* were assumed to coincide at a same point. In the Laser system *L*, when it rotates in the tilt direction, its origin moves on a circle with radius d_{AL}, around the rotation axis.

3.2.2 Marker recognition algorithm

First, an image captured by the camera is transferred into a grayscale format. The gradient of the grayscale is amplified through a logarithm transformation. Then, a 3×3 Sobel filter is used to select pixels as edge points, which have a larger gradient of grayscale than a threshold, and the image is binarized. In these edge point clusters, ellipses are detected. Finally, the marker's ID and long axis are recognized (if any), and the marker's center is seen as a feature point. [9]

3.2.3 Marker position estimation using the camera

In this algorithm, to estimate the 3D-position vector of a marker $\boldsymbol{T}_{AM}$ in the motion base system *A*, the following parameters are used: the radius of the marker pasted in environment r_{real}, the marker's position in the screen system (x_S, y_S), the major radius of the marker's image r_{image} and the camera's parameters (Internal parameters: focal length *f*, camera's CCD chip width w_{CCD}, resolution w_{reso}, h_{reso}. External parameters: camera's position $\boldsymbol{T}_{AC}$ in the motion base system *A*, pan direction c_{pan} and tilt direction c_{tilt} in the motion base system *B*). While the camera's internal parameters and $\boldsymbol{T}_{AC}$ are known in advance the direction parameters are obtained from the communication between the motion base and the PC. After setting the system on, the camera rotates automatically to recognize the markers in the environment. When a marker's image is captured by the camera, the parameters (x_S, y_S) and r_{image} are obtained through image processing.

The distance between the camera and a marker d_{CM} is estimated as shown in (3.1), where *d* is the distance between the center of the marker's image and the screen's center:

$$d_{CM} = \frac{r_{real}}{r_{image}} \sqrt{d^2 + \left(\frac{w_{reso}}{w_{CCD}} \right)^2} \tag{3.1}$$

The pan and tilt coordinates of the marker, m_{pan} and m_{tilt}, in the camera system *C*, are:

$$\begin{aligned} m_{pan} &= \frac{v_h}{w_{reso}} \left(\frac{w_{reso}}{2} - x_S \right) \\ m_{tilt} &= \frac{v_h}{w_{reso}} \left(\frac{h_{reso}}{2} - y_S \right) \end{aligned} \tag{3.2}$$

where $v_h = \arctan(w_{CCD}/2f)$

Finally, the marker's estimated 3D-position vector $\boldsymbol{T}_{AM}$, in the motion base system *A*, is:

$$\boldsymbol{T}_{AM} = \boldsymbol{T}_{AC} + \boldsymbol{R}_Z(m_{pan} + c_{pan})\boldsymbol{R}_Y(m_{tilt} + c_{tilt})\boldsymbol{D}_M \tag{3.3}$$

where $\boldsymbol{D}_M = (-d_{CM}, 0, 0)$, and $\boldsymbol{R}_Y(\alpha)$, $\boldsymbol{R}_Z(\beta)$ are rotation matrices with the angles α, β around the axis Y, Z, of the motion base system *B*, respectively.

3.2.4 Position measurement using the laser rangefinder

When the laser rangefinder is turned on, the distance between the laser dot and the laser rangefinder d_{LD} is measured. Using this distance d_{LD} and the direction parameters of the laser rangefinder in the motion base system *A* (obtained from the communication between computer and the motion base) s_{pan} and s_{tilt}, the 3D-position vector of the laser dot T_{AD} in the motion base system *A* is calculated as:

$$\boldsymbol{T}_{AD} = \boldsymbol{R}_Z(s_{pan})\boldsymbol{R}_Y(s_{tilt})\boldsymbol{D}_r \tag{3.4}$$

where $\boldsymbol{D}_r = (-d_{LD}, 0, d_{AL})$, and $\boldsymbol{R}_Y(\alpha)$, $\boldsymbol{R}_Z(\beta)$ are rotation matrices with the angles α, β around the axis Y, Z, of the motion base system *A*, respectively.

3.2.5 Markers' automatic measurement algorithm

This section describes the details about how to

automatically measure a recognized marker

1) Calculate d_{CM}, m_{pan}, and m_{tilt} of the marker as shown in (3.1) and (3.2).
2) According to the result, adjust the camera pose so that the center of the marker's image coincides with the screen's center.
3) Adjust the focal length to resize the major radius r_{image} so as to be 30% of h_{reso}. If the ratio a% of the major radius r_{image} vs. h_{reso} is smaller than 20% before adjusting the focal length, adjust the camera's focal length in order to increase the ratio from a% to 20%, and repeat the steps 1) to 3).
4) Repeat steps 1) and 2) to move the center of the marker's image to a point where it coincides again with the screen's center. Now the focal length $f_{a\%}$ is:

$$f_{a\%} = \frac{afh_{reso}}{100r} \tag{3.5}$$

Where f is the focal length and r is the major radius of marker's image when the marker was recognized. Record the marker's center (x_S, y_S) and the minor radius of marker's image b.

5) Repeat 1) to calculate d_{CM}, m_{pan}, and m_{tilt}, then calculate the vector $\boldsymbol{T}_{AM} = (x_M, y_M, z_M)$ as shown in (3.3).
6) Calculate directions t_{pan} and t_{tilt} of the marker in the motion base system A as shown in (3.6) and (3.7). Then, adjust the laser rangefinder so that it points to the marker's center, according to the result obtained.

$$t_{pan} = \arctan(y_M / x_M) \tag{3.6}$$

$$t_{tilt} = \arctan\left(\frac{z_M}{\sqrt{x_M^2 + y_M^2}}\right) \tag{3.7}$$

7) Shorten the shutter speed of the camera to reduce the brightness of the image, so that the laser dot on the image is easily detected.
8) Turn off the laser dot.
9) Save the image captured by the camera as $\boldsymbol{I}_{off}$.
10) Turn on the laser dot.
11) Save the image captured by the camera as $\boldsymbol{I}_{on}$.
12) Calculate the grayscale difference between $\boldsymbol{I}_{on}$ and $\boldsymbol{I}_{off}$, and then compute the area s_{diff} of pixels whose difference is larger than a threshold.
13) If s_{diff} is smaller than a threshold, it means that the laser dot was not found in the image; should this happen, proceed as described in step 14), otherwise skip to step 15).
14) Equi-spacedly, adjust the laser rangefinder's direction along a spire curve whose center is the direction obtained in step 6). Then repeat the steps 8) to 13). If the iteration number is larger than a threshold, the marker's measurement has failed. (Turn to the next marker's measurement.)
15) Calculate the center of gravity $\boldsymbol{G} = (x_G, y_G)$ of the pixels that were picked in step 12).
16) Calculate the relative vector between $\boldsymbol{G}$ and the center of the marker's image (x_S, y_S). If the length of the vector is larger than 1.5b (b was obtained in 4)), go back to step 14), otherwise go to 17).
17) If the length of the vector obtained in step 16) is smaller than a threshold, it means that the laser dot was shot at the marker's center, if so skip to step 19), otherwise go to 18).
18) Adjust the laser rangefinder's direction so that it points to the marker's center and go back to step 8). The adjusting parameters are calculated as shown in (3.8) and (3.9), where v_h is the horizontal view angle of camera at step 11), t'_{pan} and t'_{tilt} are the laser rangefinder's directions at step 12).

$$t_{pan} = t'_{Pan} + \left(v_h / w_{reso}\right)\left(x_G - x_S\right) \tag{3.8}$$

$$t_{tilt} = t'_{tilt} + \left(v_h / w_{reso}\right)\left(y_G - y_S\right) \tag{3.9}$$

19) Calculate the marker's position $\boldsymbol{T}_{AM}$ following the algorithm described in 3.2.4.

3.2.6 Coordinate system transformation

The coordinates of the 3D-position vector $\boldsymbol{T}_{AM}$ must be transformed into the world system. The unit vectors along the axis X, Y, Z of the world system in the motion base system A are:

$$\begin{aligned} \boldsymbol{X}_u &= \left(\boldsymbol{T}_{AM2} - \boldsymbol{T}_{AM1}\right) / \left\|\boldsymbol{T}_{AM2} - \boldsymbol{T}_{AM1}\right\| \\ \boldsymbol{Z}_u &= \boldsymbol{X}_u \times \left(\boldsymbol{T}_{AM3} - \boldsymbol{T}_{AM1}\right) / \left\|\boldsymbol{T}_{AM3} - \boldsymbol{T}_{AM1}\right\| \\ \boldsymbol{Y}_u &= \boldsymbol{Z}_u \times \boldsymbol{X}_u \end{aligned} \tag{3.10}$$

where $\boldsymbol{TB}_{AMi}$ is the 3D-position vector of marker No.i (i = 1, 2, 3) in the motion base system A. They are obtained from (3.4). Hence, the rotation matrix $\boldsymbol{R}_{WA}$ from the world system W to the motion base system A is

$$\boldsymbol{R}_{WA} = \begin{bmatrix} \boldsymbol{X}_u \\ \boldsymbol{Y}_u \\ \boldsymbol{Z}_u \end{bmatrix} \tag{3.11}$$

The translation vector $\boldsymbol{T}_{WA}$ from the world system W

to the motion base system A is given by

$$\boldsymbol{T}_{WA} = -\boldsymbol{R}_{WA}\boldsymbol{T}_{AM1} \tag{3.12}$$

The transformation matrix from the motion base system A to the world system W is

$$\boldsymbol{T}_{AW}^{44} = \begin{bmatrix} \boldsymbol{R}_{WA} & \boldsymbol{T}_{WA} \\ \boldsymbol{O} & 1 \end{bmatrix} \tag{3.13}$$

Finally, the 3D-position vector $\boldsymbol{T}_{WMi}$ of marker No.i in the world system is:

$$\begin{bmatrix} \boldsymbol{T}_{WMi} \\ \boldsymbol{1} \end{bmatrix} = \boldsymbol{T}_{AW}^{44} \begin{bmatrix} \boldsymbol{T}_{AMi} \\ \boldsymbol{1} \end{bmatrix} \tag{3.14}$$

3.3 System installation

The system's appearance is shown in Fig.4. The program and the user interface were developed by Microsoft Visual C++ 2005 on Microsoft Windows XP. During the automatic measurement some markers could fail to be measured if their positions, relative to the system, are not adequate. Should this happen, it would be necessary to measure these markers again. Note that, in this case, there is no need to measure all the markers again and that, sometimes, manual measurements may be needed. For this reason, the system includes the options of measuring only selected markers and manually measuring markers. The user interface is shown in Fig.5.

Fig.4 System's appearance.

I. Image display interface. Here, the image currently captured by the camera is displayed.
II. Marker auto-measurement interface. Here, there are the buttons to start or to cancel a marker's auto-measurement (For all markers or selected markers only).
III. Camera control box. Here, the camera can be controlled manually (pan, tilt and zoom), and the images captured by the camera can be displayed as angle maps.
IV. Laser rangefinder control box. Here, the laser rangefinder can be controlled manually (pan, tilt, laser dot on or off.)
V. Measurement status display box. Here, each marker's information is displayed (ID, 3D-position, etc.) and users can select the markers to be measured.
VI. Manual measurement control box. Here, the 3D-position of the laser dot can be measured manually.
VII. Actions log of the system.
VIII. Others. From here, the system can be initialized. Also, the time of measurement is displayed here.

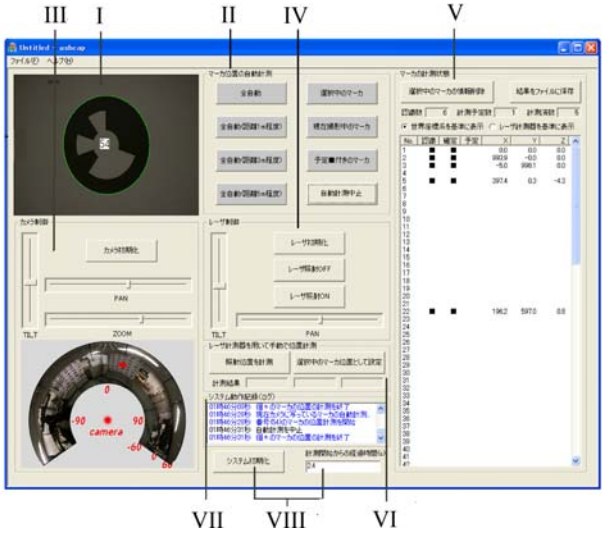

Fig.5 Program interface.

4 Performance evaluation

The performance evaluation experiment was conducted in a lab environment. In this experiment, the accuracy, stability and running time of the system were evaluated.

4.1 Experimental environment

The size of the experimental field was about 5m×5m, as shown in Fig.6. 72 circular markers, with diameter of 100mm and placed at 200mm equidistant intervals, were carefully arranged on two panels, as shown in Fig. 7. The panels' width was 1.24m and their height was 2m. The center of marker No.1, placed on the down-left corner of panel No.1, was defined as the origin. The center of marker No.2, placed on the

down-right corner of panel No.1, was located at (1000mm, 0, 0). The center of marker No.3, placed on the upper-left corner of panel No.1, was located at (0, 1000mm, 0). Consequently, the world coordinate system was defined. While panel No.1 was fixed at all times, panel No.2 was moved during the experimental process.

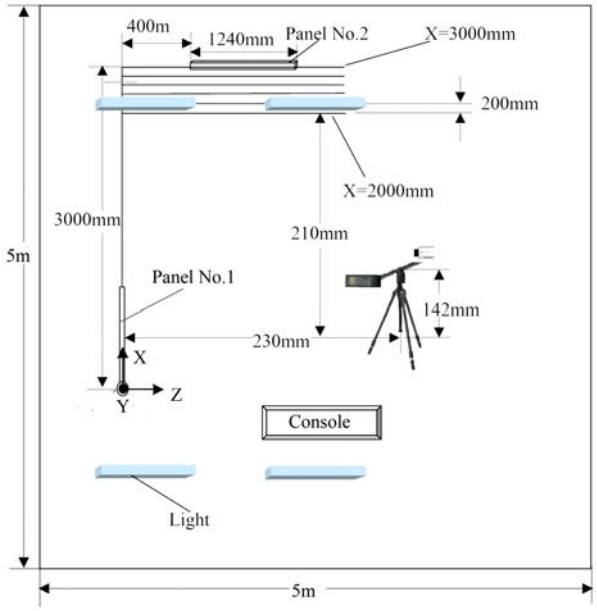

Fig. 6 Experimental environment.

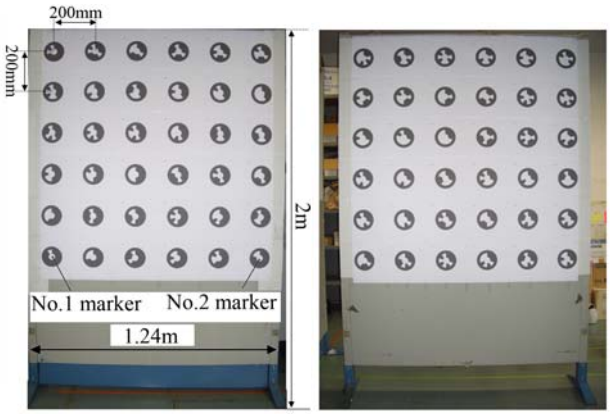

Fig. 7 Markers panel (Left: panel No.1. Right: panel No.2).

4.2 Method

Panel No.2 was placed at positions where x=2000mm, 2400mm, 2600mm, 2800mm and 3000mm, and the down-left marker on it was located at (x, 0, 400). At every position, the system's automatic measurement was repeated 20 times.

4.3 Results

Here, the system error (*SE*) and the random error (*RE*) were estimated as:

$$SE = \sqrt{(\bar{x} - x_0)^2 + (\bar{y} - y_0)^2 + (\bar{z} - z_0)^2} \quad (4.1)$$

$$RE = \sqrt{\frac{1}{n-1}\sum_{i=1}^{n}\{(x_i - \bar{x})^2 + (y_i - \bar{y})^2 + (z_i - \bar{z})^2\}} \quad (4.2)$$

where (x_0, y_0, z_0) is the real position of a marker and $(\bar{x}, \bar{y}, \bar{z})$ is the average position of the measured values. (x_i, y_i, z_i) is the i^{th} measurement position of a marker. (In total, there were n=20 measurement positions of each marker)

4.3.1 Accuracy

The system error of each marker is shown in Fig. 8 ~ 9. Of a total of 8640 results (72 markers × 6 positions of panel No.2× 20 repetitions), the maximum error between the measurement value and the real value was 27.6mm, and the average error was 7.6mm. As shown in Fig. 9, when x=2000mm on panel No.2, the error increases from the down-left corner to the upper-right corner, and it is much lager than the one found on panel No.1. The same trends of the system error on panel No.2 were found at other positions. The reason of this is that panel No.2 has a deviation from its ideal position, so the real position contains an error.

4.3.2 Stability

The random error of each marker is shown in Figs. 10 ~ 11. The trends of the random error on panel No.2 at other positions were very similar to the one detected at x=2000. The maximum value of the random error was 6.2mm and the average was 3.5mm. Since the random error was much smaller than the system error, the system error is the main error. In other words, the repetition of measurements has a little effect on the accuracy. Whether the accuracy and the stability are enough for actual field applications is discussed in 5.3.2.

4.3.3 Running time

One successful experiment (a successful automatic measure of the 72 markers) took 25.2 minutes on average. (One marker took 21.0 seconds on average). When the distance between the laser rangefinder and panel No.2 increased, the measurement time became longer. Because the accuracy of a marker's position estimation in (3.3) decreases when the distance increases, it would take more time to match the laser dot with a marker's center automatically.

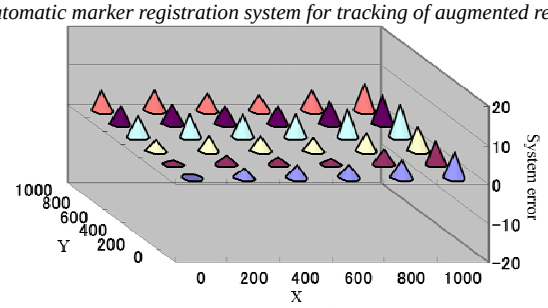

Fig. 8 System error on panel No.1 (mm).

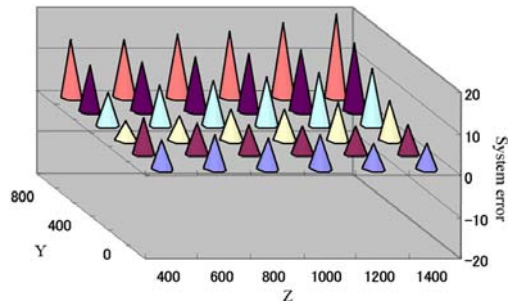

Fig. 9 System error on panel No.2, x=2000 (mm).

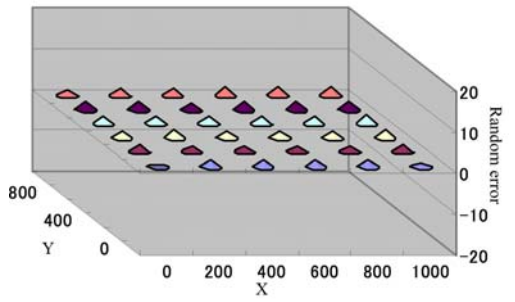

Fig. 10 Random error on panel No.1 (mm).

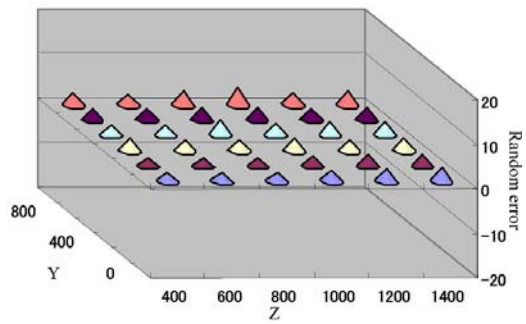

Fig.11 Random error on panel No.2, x=2000 (mm).

5 Feasibility evaluation

To evaluate the feasibility of applying this system to a NPP, an experiment was conducted in Fugen NPP. This evaluation included whether the system meets the 6 requirements mentioned at the beginning of section 3, whether it can work successfully in a NPP environment, whether NPP workers master this system quickly, and what should be improved.

5.1 Environment

The evaluation field was a pure-water chamber whose size was 9.5m×8m approximately, as shown in Fig.12. The luminance was 200-500Lux, so the markers were recognized easily.

5.2 Method

First, the system operation was demonstrated to two evaluators who had never used the system before. One of the evaluators was a Fugen NPP worker who was proficient in NPP field work (evaluator A), the other was a human interface expert (evaluator B). In order to test the system's feasibility for beginners, the two evaluators operated the system together by themselves. Three markers (No.1 to No.3) were located so as to define the world coordinate system. Another twenty markers were pasted at the objects needed for tracking, as shown in Fig.13. After the system finished the measurements, the obtained results were used in a small PC for the workers to experience an AR application. The real-time tracking of the position and orientation of the PC was performed through a camera. As shown in Fig.14, the tracking result was used in AR to display important information for the workers, such as the fluid state in the pipes (with green frame), and guidelines (with red frame). Finally, the evaluators filled a questionnaire about the feasibility of the system. Each item in the questionnaire was graded on a scale from 1 to 5 (1 - disagree, 2 – slightly disagree, 3 - neither, 4 – slightly agree, 5 - agree) and the evaluator's reasons were included, when needed.

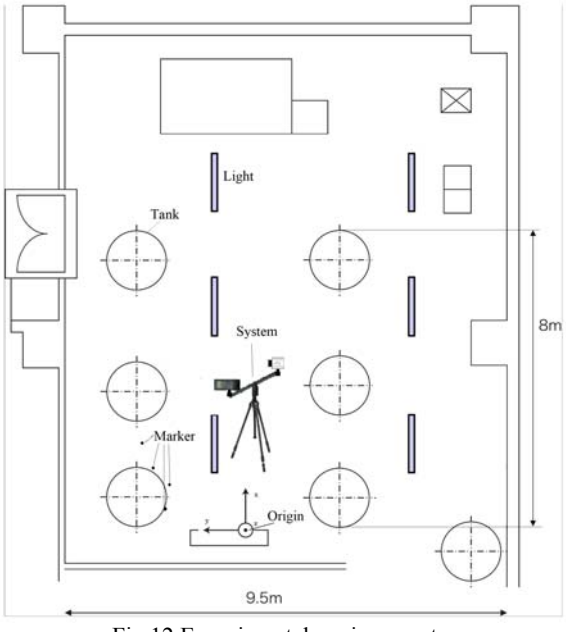

Fig.12 Experimental environment.

Fig.13 Pure-water chamber with markers.

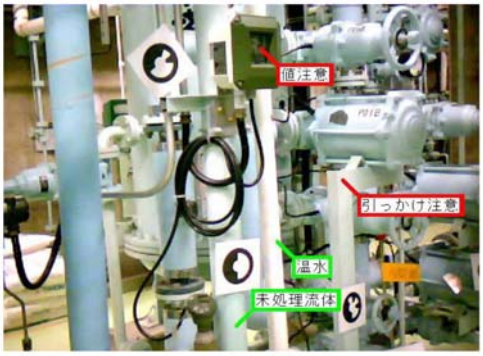

Fig.14 AR experience using the measurement results.

5.3 Results and discussion

5.3.1 Running time

It took 85 seconds to paste the markers, 350 seconds to set the system and 75 seconds to start the system. Then, 640 seconds were spent in measurements. Including the time to remove the system, 240 seconds, a total of 1390 seconds (23.2 minutes) were spent.

5.3.2 Evaluation of the system functions

The evaluation items included in the evaluation of the system functions and the obtained results are shown in Table 2 and Table 3. Items A-1 to A-5 and item A-8, which correspond to the automatic measurement functions of the system, were highly graded. This implies that the automatic measurement functions are useful when measuring. Item A-6 was given a low evaluation value. Although the evaluators thought that it was faster than any other existing measurement method, they considered that, for a practical use, the measurement speed should still be improved. Item A-7 was also given a low evaluation value. The evaluators thought that the required accuracy depends on different cases and, therefore, it was difficult to evaluate whether the accuracy was good enough. In other words, they thought that the accuracy may not be sufficient in some cases. Item A-9 was graded with

Table 2 Results of the system functions evaluation I

No.	Survey item	Result	
		A	B
A-1	When a marker is measured, the marker's automatic recognition by the camera is effective.	4	5
A-2	When a marker is measured, the automatic measurement by the laser rangefinder is effective.	4	5
A-3	When a marker is measured, the direction control by the motion base is effective.	5	5
A-4	The automatic recognition of all markers pasted in environment is effective.	5	5
A-5	The automatic measurement of all markers pasted in the environment is effective.	5	5
A-6	The time spent in the automatic measurement of the markers is considerably short.	3	4
A-7	The measurement accuracy is high enough for AR applications.	4	3
A-8	The efficiency of the preparations for AR is raised by the use of automatic measurements.	5	5
A-9	The system can be used in places with low luminance	3	4
A-10	The system can be used in environments with obstacles.	3	1
A-11	The system can be used in capacious spaces.	5	5
A-12	The system can be used in narrow spaces.	3	2
A-13	The hint sound after finishing the markers measurement is effective.	3	4
A-14	The control of the camera's pan, tilt and zoom, by a slider, is effective.	5	5
A-15	The automatic measurement of only the marker whose image is shown is effective.	5	5
A-16	The function that allows deleting the measurement result of a marker is effective.	5	5
A-17	The function that allows changing a markers' measurement status (measured or not measured) is effective.	4	5
A-18	The function that allows to change the preparatory status of a marker (to be measured or not) is effective.	3	2
A-19	The function that allows choosing the measurement results in different coordinate systems (world system or laser system) is effective.	5	5
A-20	The function of displaying the system status using words is adequate.	3	5
A-21	The system initialization is adequate.	5	1

Table 3 Results of the system functions evaluation II

No.	Survey item	Result	
		A	B
A-22	The function of using a red frame on the angle map to represent the current view range of the camera is adequate.	5	4
A-23	The function of changing the camera's direction by clicking at the angle map is adequate.	5	5
A-24	The stop function during the automatic measurements is adequate.	4	5
A-25	The automatic measurement of selected markers is adequate.	5	5
A-26	The function of displaying the total number of recognized markers is adequate.	5	5
A-27	The function of displaying the total number of markers that will be measured is adequate.	5	5
A-28	The function of displaying the total number of measured markers is adequate.	5	5
A-29	The function of displaying each marker's state (recognition, measurement and preparatory) is adequate.	5	5
A-30	The function of dividing the camera's zoom in 3 ranges to automatically measure with those ranges is adequate.	3	2
A-31	The initialization of the camera's direction is adequate.	3	2

a low evaluation value as well. The evaluators believed that the experimental environment in the NPP was very bright, being difficult to know whether the system would work in a low luminance environment. Yet, considering that the performance evaluation, mentioned in Chapter 4, was conducted in a lab environment with lower luminance than in the NPP, this item may in fact deserve a higher value. Items A-10 and A-12 were given low evaluation values. In the evaluators' opinion, the system could not be set in very narrow spaces and also some of the markers may be obstructed by obstacles, which would mean unsuccessful measurements. However, note that in such a case, the program would skip the unsuccessfully measured markers and, after finishing the measurement process, the position of the system could be rearranged so as to avoid the obstacles. Thus, the unsuccessfully measured markers could be measured again using the options of measuring only selected markers or of manually measuring markers, mentioned in Section 3.3. Nevertheless, if there are too many obstacles, the measurement efficiency would decrease. In order to solve this problem, the system miniaturization and the aid of technology to avoid pasting markers in places where there are obstacles should be applied, such as inertial sensors, natural feature points, etc. Opposite to item A-10, item A-11 was given a high evaluation value. The evaluators thought that the system could be successfully used in capacious spaces. Item A-13 was graded with a low evaluation value. Evaluator A believed that the hint sound could easily be interfered by noise; and evaluator B thought that this function was not essential. Items A-14 to A-19 correspond to the manual measurement functions. Items A-14 to A-17 and item A-19 were highly rated. Both evaluators thought that the functions were useful, especially when there were markers with unsuccessful automatic measurements. However, A-18 was very low graded because evaluators considered that this function was not very important. In items A-20 and A-21, the two evaluators gave different evaluation values, high and low, so the adequateness of these functions is not defined. Items A-22 to A-29 were highly graded, implying that these functions are useful. Finally, items A-30 and A-31 were given low values, as the evaluators thought they were not really necessary.

5.3.3 Evaluation of the system's usability

The evaluation items included in this evaluation and the obtained results are shown in Table 4. In items C-1 and C-2, which correspond to setting and removing the system, the two estimators gave different evaluation values. Considering that evaluator A, given his work experience, understands better the decommissioning work in a NPP field, his answer is more relevant. Low evaluation values in items C-1 and C-2 mean that setting and removing the system is not entirely easy. In items C-3 to C-8, corresponding to the user interface, evaluator A gave high evaluation values, whereas evaluator B graded C-4 and C-8 with low values. As a human interface expert, B's answer is more pertinent. He thought that the measurement interface was not so easy to understand for a beginner, when measuring manually. Item C-9 was low graded. The evaluators believed that it was difficult for a

Table 4 Results of the systems usability evaluation

No.	Survey item	Result	
		A	B
C-1	It is easy to set up the system.	1	4
C-2	It is easy to remove the system.	3	5
C-3	It is easy to read the words and numbers from the user interface.	4	4
C-4	It is easy to operate it manually.	5	2
C-5	It is easy to understand the interface.	5	4
C-6	It is easy to push the software buttons.	5	5
C-7	It is easy to understand the display measurement results.	5	4
C-8	It is easy to control the pan, tilt and zoom manually.	5	2
C-9	It is easy for a beginner to operate the system.	3	2
C-10	The system's response to the operation is immediate.	4	5
C-11	It is easy to understand a marker's state.	5	5
C-12	It is frustrating to operate the system.	1	1

beginner to operate the system without any manual book or previous training. Finally, items C-10 to C-12 were given high evaluation values.

5.3.4 Future improvements of the system

According to the results of the evaluations, there is room for improvement in the following aspects:

1) Improve the speed of the system's actions to shorten the measurement time.
2) Improve the measurement accuracy so that the system can be applied to a wider variety of applications.
3) Miniaturize and lighten the system.
4) Improve the user interface in order to make it easier to understand.
5) Display some help information related to the system's current actions in order to make it easier for a beginner to operate the system.

6 Conclusions

In this study, an Automatic Marker Registration System to measure the 3D-position of a circular marker, automatically and quickly, was developed, so as to reduce human error and to improve measurement efficiency. Given that circular markers as well as line markers, are suitable for the application of AR in a NPP [9], the option to measure line markers should be added into this system. In order to improve the practicality of the system, the hardware should be updated to shorten the measurement time. Additionally, measurement algorithms should be upgraded to improve the system accuracy.

Reference

[1] AZUMA, R.: A survey of augmented reality. Teleoperators and Virtual Environments, 1997, 6(4): 355-385.
[2] AZUMA, R., BAILLOT, Y., BEHRINGER, R., JULIER, S., MACINTYRE, B.: Recent advances in augmented reality. IEEE Computer Graphics and Applications, 2001, 21(6): 34-47.
[3] MAYER, J.: ARTESAS supports service and maintenance workers. http://www.inigraphics.net/press/tipics/2007/issue2/2_07a04.pdf (2008.1.31).
[4] Advanced Augmented Reality Technologies for Industrial Service Application. http://www.wzl.rwth-aachen.de/en/aa272c5cc77694f6c12570fb00676ba1.htm (2008.1.31).
[5] DAVISON, AJ., REID, ID., MOLTON, ND., STASSE, O.: Monoslam: Real-time Single Camera Slam. IEEE Transactions on Pattern Analysis and Machine Intelligence, 2007, 29(6): 1052-1067.
[6] KATO, H., BILLINGHURST, M.: Marker Tracking and HMD Calibration for a Video-based Augmented Reality Conferencing system. Proc. of 2nd Inc. Workshop on Augmented Reality. San Francisco, California: IEEE, 1999, 85-94.
[7] APPEL, M., NAVAB, N.: Registration of Technical Drawings and Calibrated Images for Industrial Augmented Reality. IEEE Workshop on application of computer version. IEEE, 2000, 48-55.
[8] ZHANG, X., GENC, Y., NAVAB, N.: Taking AR into Large Scale industrial environment: Navigation and Information access with mobile computers. IEEE Int. Symp. on Augmented Reality. IEEE, 2001, 179-180.
[9] ISHII, H., FUJINO, H., ZHIQIANG, B., SEKIYAMA, T., NAKAI, T., SHIMODA, H.: Development of Wide-Area Tracking System for Augmented Reality. 12th International on Human-Computer Interaction. 2007, 234-243.
[10] QUAN, L., LAN, Z.: Linear N-Point Camera Pose Determination. IEEE Trans. on Pattern Analysis and Machine Intelligence, 1999, 21(6): 774-780.